

N,N-Carbonyldiimidazole-Mediated Amide Coupling: Significant Rate Enhancement Achieved by Acid Catalysis with Imidazole · HCl

Emily K. Woodman, Julian G. K. Chaffey, Philip A. Hopes,* David R. J. Hose, and John P. Gilday*

AstraZeneca, Global PR&D, Avlon Works, Severn Road, Hallen, Bristol BS10 7ZE, U.K.

Abstract:

Over a series of 10 aromatic amines we show the rate of CDI mediated amidation to be significantly enhanced upon introduction of imidazole · HCl as a proton source for acid catalysis. Our work supports and provides an application for previous investigations into the imidazolium effect, thus increasing the scope of CDI as an amide-coupling reagent with aromatic amines. The influence of the relative pK_a of the amines studied on the rate of reaction was also investigated.

Introduction

N,N-Carbonyldiimidazole (CDI) is one of several commonly used reagents for coupling carboxylic acids with aliphatic or aromatic amines to form amides¹ (Scheme 1). Since its initial development as a reagent in 1960² its applicability has been shown both in small-scale research and in large-scale manufacture.³

CDI (**2**) has several benefits as an amide-coupling reagent in large-scale manufacture. It is relatively cheap and readily available in kilogram quantities, and the only byproducts are carbon dioxide and imidazole which, being relatively benign, are unlikely to cause problems on scale up (Scheme 1). These benefits make CDI (**2**) an excellent reagent for activating amide-coupling reactions at scale; however, CDI (**2**) is not without its drawbacks. Slow reaction rates between aromatic amines and the CDI intermediates⁴ have limited the scope of the reaction in the pharmaceutical and the fine chemicals industries.

CDI (**2**) was used recently for an amide coupling reaction in an AstraZeneca project. The coupling, involving two aromatic substrates, proceeded at a satisfactory rate in the laboratory, but the rate was observed to be significantly retarded upon scale up to the large-scale laboratory (LSL). Initial suggestions were that scale-up factors such as changes in rate of carbon dioxide removal and in batch water content had led to the rate retardation. The influence of carbon dioxide on the rate of a CDI-mediated amide coupling reaction has already been investigated by Vaidyanathan and co-workers,⁵ but it was thought that in

our case the reduction in water content, reducing proton availability, was the overriding factor. Following this, we initiated a work programme on a model system in order to gain a better understanding of the reaction mechanism and those factors that would affect the robustness of the process.

The mechanism for the reaction of acyl-imidazole intermediates with nucleophilic reagents has been reported,⁶ and it has been shown that significant rate improvements can be achieved through use of a cationic imidazolide intermediate (**7**) (Scheme 2) in reactions with nucleophiles.⁷ This imidazolium effect⁴ has been applied in the case of aliphatic amines and demonstrated to be beneficial to the rate of CDI-mediated amidations, due to the increased reactivity of the intermediate containing a protonated or methylated imidazole leaving group. To our knowledge there is no precedent for the application of the imidazolium effect to achieve rate enhancements in amide-coupling reactions with aromatic amines.

Consideration of the literature led us to devise a hypothesis that the addition of a weakly acidic compound to the amide coupling reaction would have two advantageous effects. First, it would act as a proton source that is required in the proton transfer steps, and second it would result in the partial protonation of the imidazolide (**3**), leading to the more reactive intermediate (**7a**). Therefore, the weakly acidic compound would not only lead to the required increased rate of reaction, but it would also result in a more robust process. Whilst the option of using methylating agent, such as methyl iodide, was considered, it was not pursued as Jencks and co-workers have previously shown that methylated and protonated intermediates are equivalent in the case of weakly nucleophilic amines.^{6,7} In addition, it is desirable to avoid the use of toxic alkylating reagents such as methyl iodide.

Our choice of weakly acidic compound was required to meet a number of criteria: it had to be cheap and readily available in kilogram quantities; it must be easily removed from the reaction mixture with little or no modifications to the current work-up procedure; it must not lead to the formation of impurities that may affect the downstream chemistry; and finally it must be acidic enough to increase the concentration of the protonated intermediate (**7a**), but not sufficiently acidic to significantly protonate the nucleophilic amine. To this end, imidazole · HCl was selected as it meets all of the above requirements and imidazole is already present in the reaction mixture. We hypothesised that the aqueous disassociation constant of imidazole · HCl ($pK_a = 7.0$)⁸ would be sufficiently acidic to

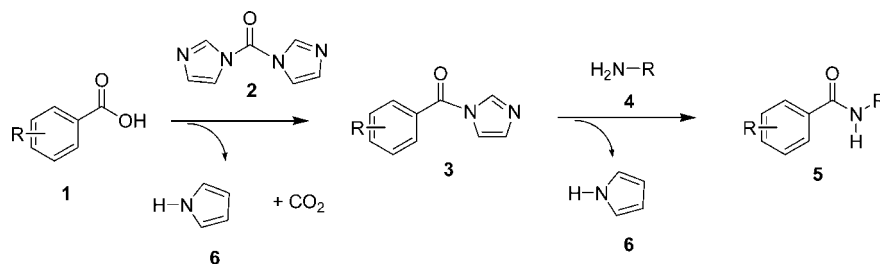
* To whom correspondence should be addressed. Telephone: +44 117 9385456. Fax: +44 1179385081. E-mail: Philip.Hopes@astrazeneca.com; John.Gilday@astrazeneca.com.

(1) Montalbetti, C.A.G. N.; Falque, V. *Tetrahedron* **2005**, *61*, 10827.
 (2) Paul, R.; Anderson, G. W. *J. Am. Chem. Soc.* **1960**, *82* (17), 4596.
 (3) Dale, D. J.; Dunn, P. J.; Golightly, C.; Hughes, M. L.; Levett, P. C.; Pearce, A. K.; Searle, P. M.; Ward, G.; Wood, A. S. *Org. Process Res. Dev.* **2000**, *4*, 17.
 (4) Grzyb, J. A.; Shen, M.; Yoshina-Ishii, C.; Chi, W.; Stanley Brown, R.; Batey, R. A. *Tetrahedron* **2005**, *61*, 7153.
 (5) Vaidyanathan, R.; Kalthod, V. G.; Ngo, D. P.; Manley, J. M.; Lapekas, S. P. *J. Org. Chem.* **2004**, *69*, 2565–2568.

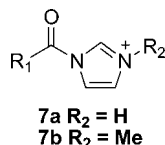
(6) Oakenfull, D. G.; Salvesen, K.; Jencks, W. P. *J. Am. Chem. Soc.* **1971**, *93*, 188.

(7) Wolfenden, R.; Jencks, W. P. *J. Am. Chem. Soc.* **1961**, *83*, 4390.

Scheme 1



Scheme 2



partially protonate the imidazolide intermediate (**3**) (predicted $pK_a = 3.7$)⁹ whilst ensuring sufficient unprotonated amine was present to carry out efficient nucleophilic attack.

We chose to investigate a series of 10 aromatic and heteroaromatic amines (Table 1) that span 12 pK_a units (based upon aqueous pK_a predictions), which would cover a range of reaction rates. This gave us the opportunity to investigate both the effect of using imidazole·HCl for acid catalysis and the influence of the amine, or more specifically the pK_a of the amine on the reaction. This paper reports the results of our investigations into these 10 amines (Table 1).¹⁰

Results and Discussion

Each amine was investigated by carrying out the amidation reaction with benzoic acid (**8**) in two steps (Scheme 3). In the first step the imidazolide intermediate (**3**) was formed in greater than 97% conversion. The reaction mixture was then heated to 50 °C before the addition of the amine (**4**). The progress of the amidation reaction was monitored by HPLC, using a butylamine quench to facilitate analysis. In each case the reaction was carried out both with and without acid catalysis in order to give a direct comparison of rates. NMP was used as the reaction solvent for all reactions to ensure complete dissolution of all reactants and intermediates. Figure 1 shows a representative example of the results collected.¹¹

Figure 1 demonstrates a significant decrease in reaction lifetime on changing the noncatalysed reaction conditions (~5 days) to those with acid catalysis (~5 h). All of the reactions involving anilines follow analogous reaction profiles, although

the results for the heterocyclic amines deviate from the trend. Table 2 lists each of the amines studied together with the lifetimes (defined as time to >90% conversion by quantitative HPLC) of their reactions with benzoic acid both with acid catalysis and without acid catalysis at 50 and 100 °C where applicable.

Using numerical methods,¹² the rate constants for the reactions of each amine under both acidic and nonacidic conditions were determined (Table 3). It has been assumed for the purposes of fitting the data that the reactions obey second-order kinetics.

Only the results from the series of anilines (**4a–4g**) will be considered initially, ignoring the heterocycles (**4h–4j**). Throughout the series of anilines the rate constant is seen to increase by 20-fold on average when the reaction is carried out under acid catalysis compared to being carried out without acid catalysis. This difference in rate demonstrates that using imidazole·HCl as a proton source for acid catalysis in CDI-mediated amide-coupling reactions does lead to an increase in the rate of reaction between the imidazolide intermediate and the amine within this series of anilines. The Brønsted-type plot (Figure 2) demonstrates strong correlation between the aqueous pK_a of the anilines and their corresponding logarithmic rates of reaction.

The plot shows clearly that the rate of reaction, both in the catalysed and uncatalysed cases, decreases as the pK_a of the amine decreases, reflecting the decreasing nucleophilicity of the amine. The strong correlation ($R^2 > 0.97$) in each of the cases suggests that across the series of anilines the mechanism and rate-determining step of the reaction is consistent. However, the fact that the two correlations are distinct implies that the rate-determining step differs between the two sets of conditions. These observations support our suggestion that one rate-determining step, in the presence of imidazole·HCl, is controlled by the protonated intermediate, whereas the other, without imidazole·HCl present, is not.

Whilst the results for the anilines clearly show an increase in reaction rate when the reaction is carried out with acid catalysis, the results for the heterocyclic amines are not as conclusive. The rate of reaction increases by an order of magnitude with acid catalysis compared to the rate of the uncatalysed reaction in the case of 4-aminopyrimidine (**4h**), which is consistent with the trend seen in the anilines. However, in the case of 4-aminopyridine (**4j**) the trend is reversed, and the rate of reaction is seen to decrease by 6-fold under acid

(8) Bonvicini, P.; Levi, A.; Lucchini, V.; Modena, G.; Scorrano, G. *J. Am. Chem. Soc.* **1973**, *95*, 5960.

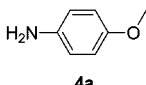
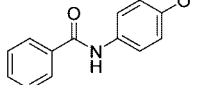
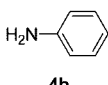
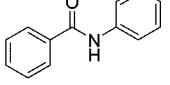
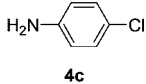
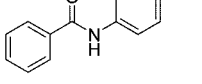
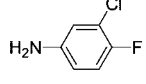
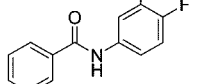
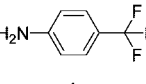
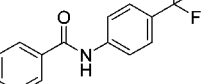
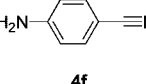
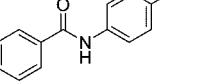
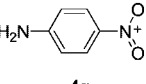
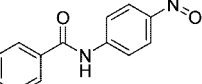
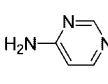
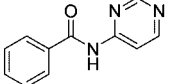
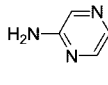
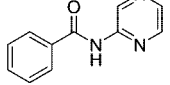
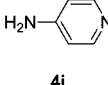
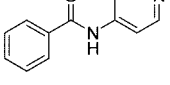
(9) *ACD Labs pKa Database, Version 10.01*; Advanced Chemistry Developments Inc.: Toronto, Canada, 2007.

(10) References for quoted pK_a 's: (a) Willi, A. V.; Meirer, W. *Helv. Chim. Acta* **1956**, *39*, 318. (b) Bolton, P. D.; Hall, F. M. *Aust. J. Chem.* **1967**, *20*, 1797. (c) Bolton, P. D.; Hall, F. M. *J. Chem. Soc.* **1969**, *B*, 259. (d) *ACD Labs pKa Database, Version 10.01*; Advanced Chemistry Developments Inc.: Toronto, Canada, 2007. (e) Sheppard, W. A. *J. Am. Chem. Soc.* **1962**, *84*, 3072. (f) Fickling, M. M.; Fischer, A.; Mann, B. R.; Packer, J.; Vaughan, J. *J. Am. Chem. Soc.* **1956**, *81*, 4226. (g) Gold, V.; Tomlinson, C. *J. Chem. Soc.* **1971**, *B*, 1707. (h) Fischer, A.; Galloway, W. J.; Vaughan, J. *J. Chem. Soc.* **1964**, 3591. (i) Bender, M.; Chow, Y. *J. Am. Chem. Soc.* **1959**, *81*, 3929. (j) Albert, A.; Goldacre, R.; Phillips, J. N. *J. Chem. Soc.* **1948**, 2240.

(11) A full set of reaction profiles can be found in the Supporting Information.

(12) The fitting of the experimental data was performed using *Dynochem version 3.2.1.0*; Performance Fluid Dynamics (P.F.D.) Limited: Dublin, Ireland, 2007.

Table 1. Amines investigated together with their aqueous pK_a 's and the amides formed

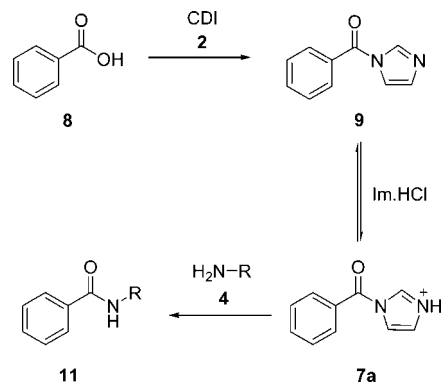
Amine	Aqueous pK_a	Amide
	5.36	
4a		11a
	4.60	
4b		11b
	3.98	
4c		11c
	3.60	
4d		11d
	2.75	
4e		11e
	1.74	
4f		11f
	1.00	
4g		11g
	-4.88 (5.69) ^a	
4h		11h
	-4.40 (3.00) ^a	
4i		11i
	-6.30 (9.12) ^a	
4j		11j

^a Value in parentheses refers to the pK_a of the ring nitrogen.

catalysis, implying that the proton source is retarding the reaction rate rather than accelerating it.

No rate constants are reported for 2-aminopyrazine (**4i**) as, at 50 °C, no reaction was seen either with or without acid catalysis over a 6-day period. It seems that under the conditions

Scheme 3



chosen **4i** is simply too unreactive. However, by increasing the reaction temperature to 100 °C the reaction could be driven to completion within 24 h with acid catalysis (6 times faster than without acid catalysis).

The clear correlations seen between pK_a and reaction rate in the Brønsted-type plot shown in Figure 2 are lost if the heterocyclic amines are included. The loss of correlation could imply that the heterocyclic amines react *via* a different rate-determining step from that of the anilines.

The Hammett plot¹³ (Figure 3) for the series of anilines shows a reasonable linear relationship for both the acidic and nonacidic processes. The 3-chloro-4-fluoroaniline is an obvious and unexplained outlier. The gradients of the regression lines, corresponding to ρ of the Hammett equation, are both negative (-3.66 and -3.56 for the acidic and nonacidic processes, respectively), indicating that electron-donating groups on the aniline increases the rate of reaction through the stabilisation of the developing positive charge at the reactive centre in the transition state. The values of ρ are not dissimilar to ρ obtained for the reaction of a series of anilines with benzoyl chloride in benzene at 25 °C ($\rho = -2.69$).¹⁴ The very similar values of ρ obtained for the acidic and nonacidic processes suggest that, from the perspective of the aniline, the reaction mechanism is virtually identical in both regimes. This lends additional support that the acidic conditions activate the benzoyl imidazolide to attack (Table 4).

During our work, we have assumed that the imidazolium effect proposed by Jencks, and named as such by Batey, is correct. We decided to explore this further through density functional theory (DFT) calculations. In principle the benzoyl imidazolide could protonate either on the nitrogen atom (**7a**) or the carbonyl oxygen (**12**) (Scheme 4). Either structure would activate the carbonyl group to nucleophilic attack.

The gas-phase proton affinities¹⁵ of benzoyl imidazolide (**9**) were calculated¹⁶ at the B3LYP/6-31+G**/B3LYP/6-31G* level of theory. The results obtained indicate that the protonation of the nitrogen atom is preferred (940.7 kJ mol⁻¹) over protonation of the carbonyl oxygen (827.2 and 833.9 kJ mol⁻¹ for the *Z*-

(13) Hammett, L. P. *Chem. Rev.* **1935**, *17* (1), 125.

(14) Sykes, P. *A Guidebook to Mechanism In Organic Chemistry*, 6th ed.; Longman Group Ltd.: Harlow, 1986; p 364.

(15) The proton affinity is defined as the negative of the enthalpy change in the gas-phase reaction between a proton and the chemical species concerned, usually an electrically neutral species, to give the conjugate acid of that species.

(16) See Supporting Information for more details of the calculations.

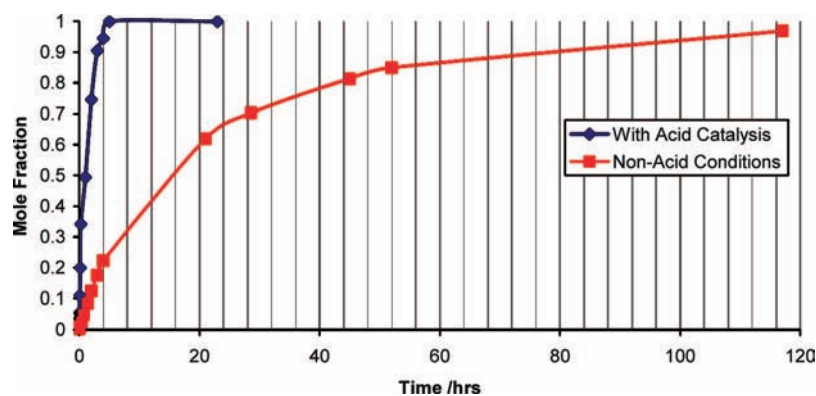


Figure 1. Reaction profile showing amide formation over time for amine 4d.

Table 2. Experimental reaction times

amine	temperature (°C)	reaction time (h) ^a	
		non-acid catalysis	acid catalysis
4a	50	1	0
4b	50	23	1
4c	50	27	2
4d	50	45	3
4e	50	175	29
4e	100	ND	3
4f	50	>>143	143
4f	100	ND	10
4g	50	>>211	>143
4g	100	ND	22
4h	50	>>211	143
4h	100	ND	23
4i	100	140	25
4j	50	114	>120

^a Reaction time to greater than 90% conversion. ND = Not Determined.

and the *E*-oxonium ions respectively). The energy difference of over 100 kJ mol⁻¹ indicates that the protonation of the oxygen is virtually insignificant compared to that of the nitrogen atom of the imidazole ring.

The Brønsted-type and Hammett plots show clear correlations with the reaction rate for the anilines studied. However, the heterocyclic amines do not obey these simple models. As such we decided to examine a multiparameter, quantitative structure activity relationship (QSAR) approach, which could be used to predict the rates of reaction of all amines studied, supporting our emphasis on improving the scope of CDI.

The geometry of each amine in turn was optimised at the B3LYP/6-31G* level of theory. From these geometries

Table 3. Rate constants calculated for reactions at 50 °C

amine		rate constant (mol/L·s)		log (rate constant)	
		non-acidic	acidic	non-acidic	acidic
4-methoxyaniline	4a	3.808 × 10 ⁻³	4.043 × 10 ⁻²	-2.42	-1.39
aniline	4b	1.802 × 10 ⁻⁴	4.649 × 10 ⁻³	-3.74	-2.33
4-chloroaniline	4c	3.129 × 10 ⁻⁵	1.016 × 10 ⁻³	-4.50	-2.99
3-chloro-4-fluoroaniline	4d	2.627 × 10 ⁻⁵	4.978 × 10 ⁻⁴	-4.58	-3.30
4-trifluoromethylaniline	4e	5.996 × 10 ⁻⁶	5.269 × 10 ⁻⁵	-5.22	-4.28
4-cyanoaniline	4f	3.678 × 10 ⁻⁷	1.084 × 10 ⁻⁵	-6.43	-4.96
4-nitroaniline	4g	1.545 × 10 ⁻⁷	3.797 × 10 ⁻⁶	-6.81	-5.42
4-aminopyrimidine	4h	2.902 × 10 ⁻⁷	2.967 × 10 ⁻⁶	-6.54	-5.53
4-aminopyrazine	4i	ND ^a	ND	ND	ND
4-aminopyridine	4j	2.527 × 10 ⁻⁵	4.042 × 10 ⁻⁶	-4.60	-5.39

^a ND = Not Determined.

quantum mechanically (QM) derived descriptors were obtained that represent aspects of the nucleophilicity of the amine. The following descriptors relating to the nucleophilic nitrogen atom were considered: partial atomic charge, the occupancy and percentage of *s*-orbital character of the lone-pair, molecular electrophilicity and softness, as well as the condensed atom electrophilicity and softness indices. The relationship between the logarithmic rate of reaction and the QM-derived descriptors was examined using the projection of latent structures (PLS) modelling technique. Four models were built that examined the acidic and nonacidic regimes for all of the compounds and the aniline subset. All four models were refined through cross-validation and model validation techniques to produce single-component models with high *R*² and *Q*² values.

Figure 4 shows that virtually identical loadings plots were obtained for the PLS models of the anilines under both acidic and nonacidic conditions, indicating that the descriptors have equal significance under each regime. This suggests that the addition of imidazole·HCl to the reaction mixture does not unduly modify the intrinsic reactivity of the anilines compared to that of the uncatalysed reaction, further supporting interpretation of the Hammett plots above.

The PLS model encompassing both the anilines and heterocyclic amines under nonacidic conditions is broadly similar to those obtained for the anilines alone, the most noticeable difference is in the loading for the percentage *s*-orbital character.

The model that is most strikingly different is the one obtained under acidic conditions, which includes both the anilines and

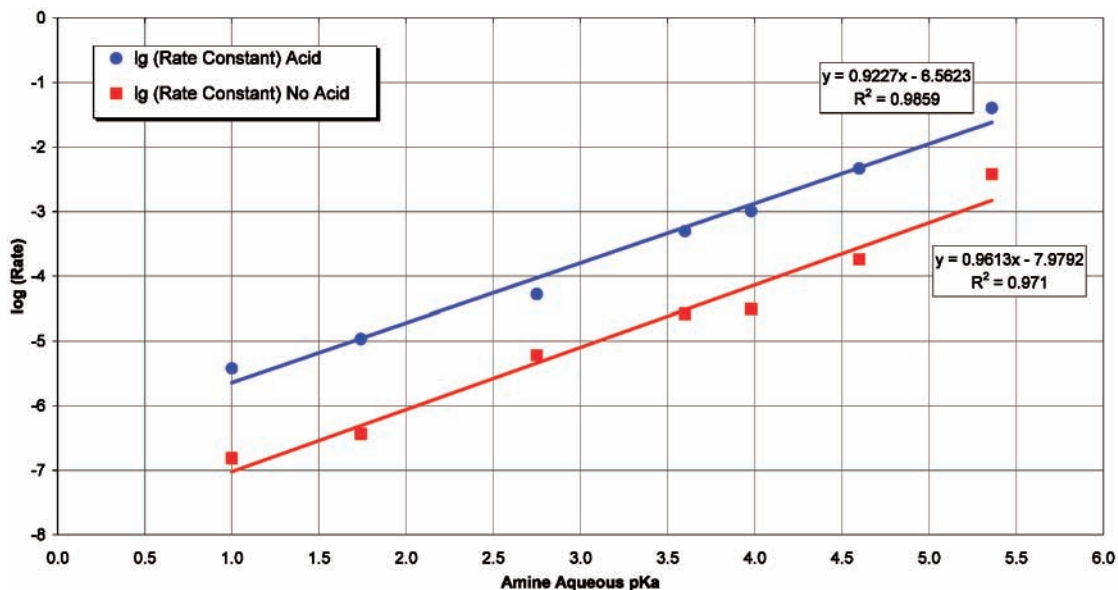


Figure 2. Brønsted-type plot for the aniline series.

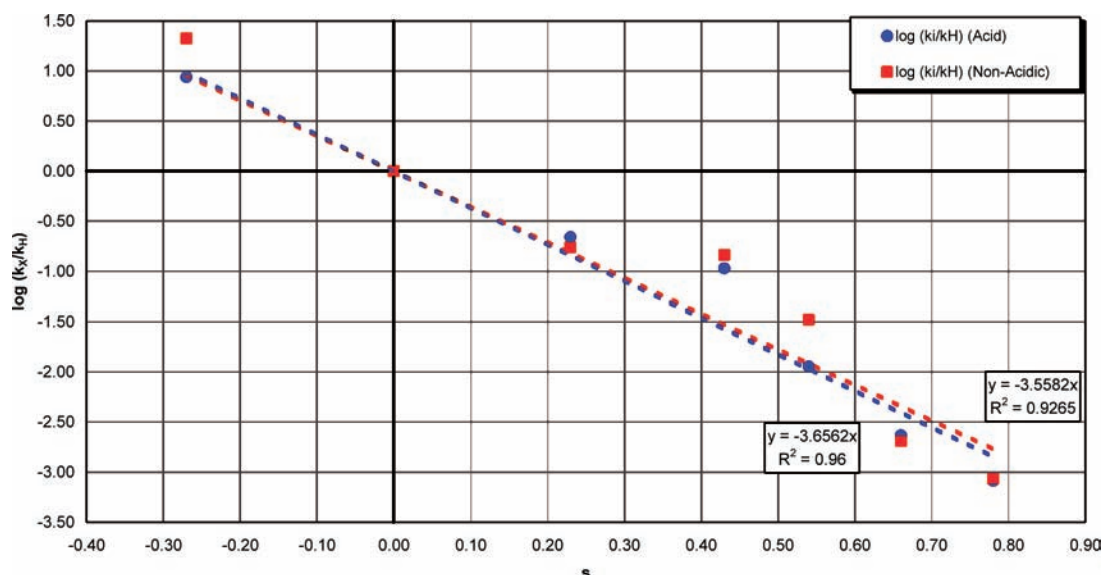


Figure 3. Hammett plot for the aniline series.

Table 4. Hammett plot parameters

amine	σ value ^a	log (k_X/k_H)	
		acidic	nonacidic
4-methoxyaniline	-0.27	0.94	1.32
aniline	0.00	0.00	0.00
4-chloroaniline	0.23	-0.66	-0.76
3-chloro-4-fluoroaniline	0.43 ^b	-0.97	-0.84
4-trifluoromethylaniline	0.54	-1.95	-1.48
4-cyanoaniline	0.66	-2.63	-2.69
4-nitroaniline	0.78	-3.09	-3.07

^a σ values used were obtained from ref 18. ^b The σ value used is the sum of the σ_{p-Cl} and σ_{m-F} .

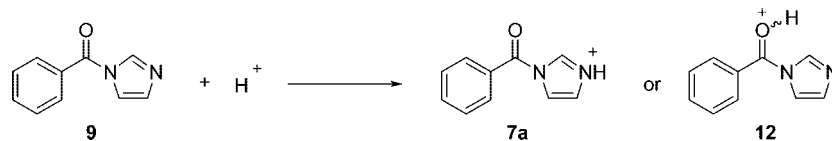
heterocyclic amines. The refined model does not include the descriptors directly relating to the nitrogen lone-pair (occupancy and s-orbital character), suggesting that as a complete group the addition of acid has an effect on the nucleophilicity of the amine as the regime changes. As demonstrated in the Hammett plot, there is no effect upon the ability of the anilines to act as

nucleophiles upon adding acid to the system, indicating that the heterocyclic amines do not fit the previously observed model.

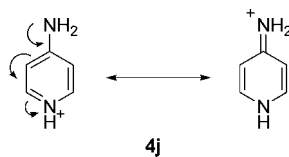
This behaviour can be readily explained in terms of the pK_a of the nitrogen atoms in the heterocycle (Table 1). The aqueous disassociation constant of the heterocyclic nitrogen in 4-aminopyridine is 9.12, indicating that in the presence of the imidazole·HCl the ring nitrogen is protonated (Scheme 5). This will result in the exocyclic nitrogen donating electron density into the ring to stabilise the positive charge; thus, the exocyclic nitrogen will have a lower propensity to undergo nucleophilic attack. The QM descriptors fail to describe this behaviour correctly, as the descriptors were calculated for the neutral and not the protonated form.

Overall the models generated under the QSAR approach support the experimental results obtained and provide a useful model in the case of the anilines (within the pK_a range studied). However, it can be seen that the heterocycles do not fit the

Scheme 4



Scheme 5



aniline model and further work would be required, covering a wider range of heterocycles in order to develop an alternative, more appropriate model.

Having investigated the properties of the nucleophile we felt that it would be useful to understand further the effect of acid concentration on the rate of reaction. As such we undertook a further experiment to demonstrate the change in rate as the concentration of imidazole·HCl is changed. Using 4-chloroaniline (**4c**) as a typical aniline, we designed an experiment to

investigate how the rate of reaction changes as the number of equivalents of imidazole·HCl is varied between 0 and 2 in 0.5 increments. For efficiency we carried out this final study using an automated reaction system,¹⁷ which allowed us to investigate the different reactions simultaneously. Although this forced us to vary the conditions away from those used in the rest of this paper, we were able to generate a self-consistent set of data across five different concentrations of imidazole·HCl. As before, we made the assumption that the reaction followed second-order kinetics in order to fit rate constants to the data.

From Figure 5, using the chosen aniline, it can be seen that the rate of reaction increases linearly with the initial charge of imidazole·HCl. This is consistent with the overall rate equation for the reaction being dependent upon acid concentration derived from the imidazole·HCl charge and that **7a** forms part of the

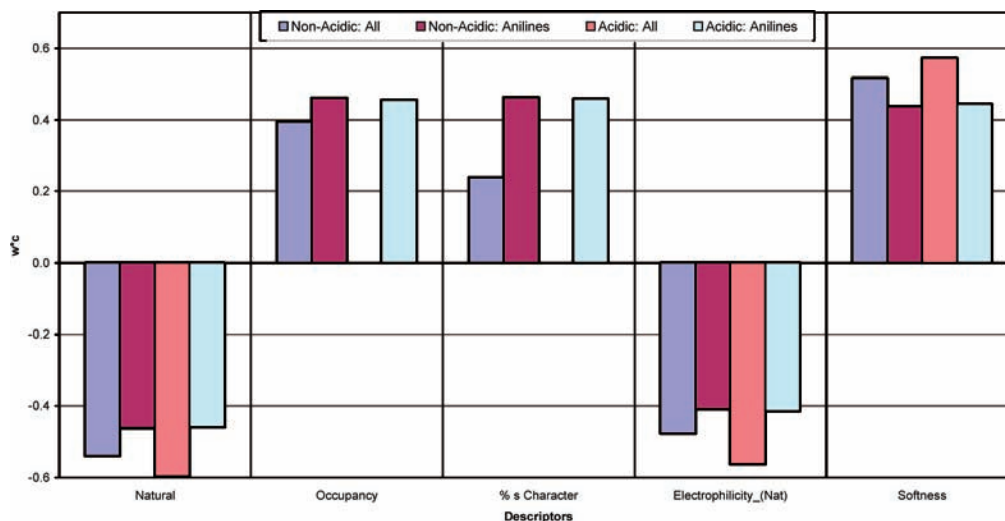


Figure 4. Summary plot of PLS loadings.

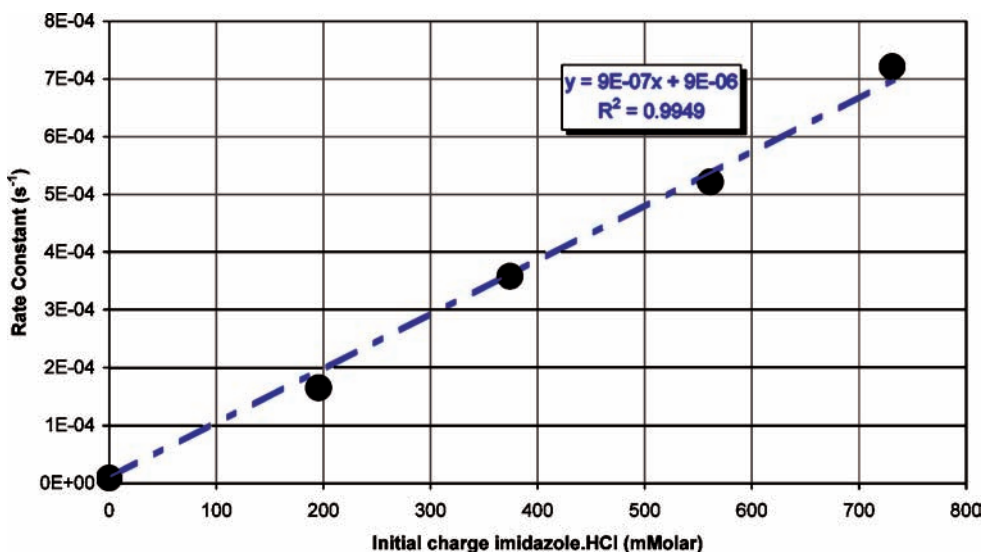


Figure 5. Change in rate with initial charge of imidazole·HCl.

rate-determining step for the reaction. Together with the evidence from the Hammett plot discussed above this leads us to the conclusion that changing from a nonacidic regime to an acidic regime enhances the rate by increasing the concentration of **7a** present without adversely affecting the level of unprotonated amine.

The linear relationship obtained supports our hypothesis that only a small proportion of the imidazolide is protonated under these reaction conditions. Whilst additional rate enhancements may be possible, we have restricted our investigation to practical imidazole·HCl charges.

Conclusions

Over the series of anilines screened, we have demonstrated that the use of imidazole·HCl significantly enhances the rate of reaction. This observation supports previous investigations into the imidazolium effect and suggests that protonation *in situ* can be used effectively to increase the rate of reactions between aromatic amines and the imidazolide intermediate generated in CDI-mediated amidations. The anilines follow the trend of increasing reaction rate with increasing aqueous pK_a , when reacting with the benzoyl imidazolide intermediate under either acidic or nonacidic conditions. Furthermore, the logarithmic rate constants for anilines can be modelled using quantum mechanically derived descriptors under acidic and nonacidic regimes.

In conclusion we have shown that reactions, which under standard conditions can take days to reach completion, can now be carried out in a matter of hours upon addition of imidazole·HCl. Crucially, for large-scale manufacture this rate enhancement can be achieved without the need for more forcing conditions, thus maximising throughput for an otherwise slow reaction with minimum impact on cost.

Experimental Section

General Considerations. All reagents were purchased from commercial sources and used without any additional purification. All experiments were carried out under a nitrogen atmosphere to maintain anhydrous conditions. The reaction profiles were followed quantitatively by HPLC on a Hewlett-Packard series 1100 machine using a Hichrom ACE Phenyl 50 mm × 3.0 mm × 3 μm column at 45 °C; flow rate: 1.25 mL/min; injection volume: 2 μL; detection wavelength: 220 nm; mobile phase 5% methanol in water increasing to 95% methanol in water over a 6 min period, 95% methanol in water was then held for 1.5 min. Both the water and the methanol eluent contained 0.03% trifluoroacetic acid. *m*-Terphenyl was used as an internal standard for the HPLC analysis, and all measurements were made within a previously defined linearity range. ¹H NMR and ¹³C NMR spectra were recorded on a Varian Inova NMR 400 MHz spectrometer operating at 399.9 MHz in DMSO-*d*₆ for ¹H NMR and 100.55 MHz for ¹³C NMR. The chemical shifts, δ, were recorded relative to tetramethylsilane as an internal standard; all coupling constants, *J*, are reported in Hz. All compounds were standardised against 2,3,5,6-tetrachloronitrobenzene (TCNB) by ¹H NMR. GC/MS was recorded on Agilent Micromass GC-TOF. IR was recorded on a Perkin-Elmer UTAR spectrometer.

Generic Experimental Procedure. Without Acid Catalysis. Benzoic acid (Aldrich >99.5%) (**8**, 1.00 g, 8.19 mmol); CDI (Acros 97%) (**2**, 1.3 equiv, 1.76 g, 10.65 mmol); *m*-terphenyl (Aldrich >98%) (200 mg, 0.86 mmol) and anhydrous NMP (Aldrich 99.5%) (20 mL, 20 rel vols) were charged to a clean, dry, three-necked, round-bottomed, 100 mL flask, fitted with an overhead stirrer (200 rpm), nitrogen bubbler, and thermometer. The reaction was allowed to proceed at ambient temperature until at least 97% conversion to the imidazolide intermediate (**9**) was achieved based upon HPLC. Samples were prepared for analysis by taking a 50 μL aliquot from the reaction mixture, quenching it in 200 μL of butylamine. After holding the quench mixture at ambient temperature for 5 min it was diluted to 50 mL with 3:1 methanol/water and then analysed using the HPLC method described above.¹⁷ Upon reaching >97% conversion, the reaction liquor was heated to 50 °C, and the appropriate amine (all sourced from Acros or Aldrich >98%) (**4**) (12.28 mmol, 1.5 equiv) was charged. Samples were then taken using the method described above at regular time intervals chosen according to the expected lifetime of the reaction.

With Acid Catalysis. The reaction conditions were the same as the uncatalysed reaction except that imidazole·HCl (Aldrich 98%) (1.76 g, 12.28 mmol, 1.5 equiv) was charged to the reaction at the same time as the benzoic acid.

Work-Up. The reaction mixtures were drowned out into water (20 mL) at ambient temperature. The precipitated white solid was isolated by filtration and dried under vacuum at 40 °C. The dry solid was recrystallised from the minimum amount of hot absolute ethanol and isolated by filtration at ambient temperature. The white crystalline solid was dried under vacuum at 40 °C. With the exception of two, all the amides synthesised in the course of this study are known and characterised in the literature. The two novel compounds synthesised have been fully characterised, and the details are listed below. In the case of the known compounds structural identity was confirmed by ¹H NMR; characterisation references for these compounds can be found in Table 4.

4h N-Pyrimidin-4-ylbenzamide: HPLC RT 2.98 min; mp 97–98 °C; ¹H NMR (399.89 MHz, DMSO-*d*₆) δ 11.22 (1H, s), 8.93 (1H, s), 8.70 (1H, d, *J*=5.6 Hz), 8.19 (1H, d, *J*=6.8 Hz), 8.00 (2H, d, *J*=8.4 Hz), 7.60 (1H, m), 7.51 (2H, m); ¹³C NMR: (100.55 MHz, DMSO-*d*₆) δ 167.62, 158.38, 158.23, 133.40, 132.62, 128.64, 128.36, 126.09, 110.77; GC/MS-EI (*m/z*): Calcd for C₁₁H₉N₃O 199.0744 (M⁺) found 199.0738 (M⁺). IR (ATR) 1682, 1568, 1504, 1459, 1394, 1308, 1265, 1176, 1112, 1072, 1024, 997, 926, 897, 866, 834, 789, 718, 689, 663 cm⁻¹.

4i N-Pyrazin-5-ylbenzamide: HPLC RT 2.90 min; mp 145–147 °C; ¹H NMR: (399.89 MHz, DMSO-*d*₆) δ 11.12 (1H, s), 9.43 (1H, d, *J*=1.6), 8.49 (1H, m), 8.43 (1H, m), 8.06 (2H, m), 7.63 (1H, m), 7.54 (2H, m); ¹³C NMR: (100.55 MHz, DMSO-*d*₆) δ 166.15, 149.05, 142.55, 139.94, 137.47, 133.36, 132.25, 128.39, 128.15; GC/MS-EI (*m/z*): Calcd for C₁₁H₉N₃O

(17) The imidazolide intermediate (**3**) was not suitable for analysis by HPLC; addition of the imidazolide intermediate to butylamine facilitated analysis of the imidazolide by reacting to form the butyl amide derivative, which was easily detected by HPLC.

(18) Hansch, C.; Leo, A.; Taft, R. W. *Chem. Rev.* **1991**, *91* (2), 165.

199.0744 (M⁺) found 199.0718 (M⁺). IR (ATR) 1671, 1530, 1410, 1292, 1258, 1054, 1010, 841, 801, 707 cm⁻¹.

Experimental Procedure Investigation in the Automated Reactor, SK233. *N*-Benzoylimidazole (Alfa Aesar 96%) (**9**, 7.06 g, 41.0 mmol), imidazole (Acros >99%) (2.79 g, 1 equiv, 41.0 mmol), and *m*-terphenyl (1.06 g, 4.5 mmol) were made up into 100 mL of stock solution with anhydrous NMP. The stock solution was then divided into five 20 mL portions and charged into five clean dry reaction tubes. Imidazole. HCl was charged to the tubes as follows; Tube A: 0 g, 0 equiv; Tube B: 0.44 g, 4.10 mmol, 0.5 equiv; Tube C: 0.87 g, 8.20 mmol, 1 equiv; Tube D: 1.31 g, 12.30 mmol, 1.5 equiv; Tube E: 1.74 g, 16.40 mmol, 2 equiv. The tubes were then set up in the SK233 instrument and heated to 46 °C. 4-Chloroaniline (**4c**, 16 g, 61.5 mmol) was made up into a 20 mL stock solution with anhydrous NMP; this solution was then charged in 2.5 mL aliquots to each of the five reaction tubes. The SK233 was programmed to sample the reaction tubes at regular time intervals after the amine charge. The sampling protocol was as follows: take 50 μL aliquot from the reaction tube and quench it into 200 μL of

butylamine; after a 5 min hold take a 50 μL aliquot from the quench and charge it into 1.5 mL of 3:1 methanol/water. The samples collected were then analysed using the HPLC method described above.¹⁶

Acknowledgment

We thank Jonathan Moseley for his help in the preparation of this manuscript. We also thank Ian Derrick for his support and advice in running the SK233. We thank Gordon Plummer and Richard Wisedale for additional analytical support.

Supporting Information Available

Complete set of graphs to complement Figure 1, and a further explanation of the computational work undertaken. This information is available free of charge via the Internet at <http://pubs.acs.org>.

Received for review September 12, 2008.

OP800226B